Powerful Organic Molecular Oxidants and Reductants Enable Ambipolar Injection in a Large-Gap Organic Homojunction Diode

Hannah L. Smith, Jordan T. Dull, Swagat K. Mohapatra, Khaled Al Kurdi, Stephen Barlow, Seth R. Marder, Barry P. Rand, and Antoine Kahn*

Cite This: *ACS Appl. Mater. Interfaces* 2022, 14, 2381−2389

Read Online

ACCESS | 📊 Metrics & More | 📖 Article Recommendations | 🆘 Supporting Information

ABSTRACT: Doping has proven to be a critical tool for enhancing the performance of organic semiconductors in devices like organic light-emitting diodes. However, the challenge in working with high-ionization-energy (IE) organic semiconductors is to find p-dopants with correspondingly high electron affinity (EA) that will improve the conductivity and charge carrier transport in a film. Here, we use an oxidant that has been recently recognized to be a very strong p-type dopant, hexacyano-1,2,3-trimethylene-cyclopropane (CN6-CP). The EA of CN6-CP has been previously estimated via cyclic voltammetry to be 5.87 eV, almost 300 meV higher than other known high-EA organic molecular oxidants. We measure the frontier orbitals of CN6-CP using ultraviolet and inverse photoemission

spectroscopy techniques and confirm a high EA value of 5.88 eV in the condensed phase. The introduction of CN6-CP in a film of large-band-gap, large-IE phenyldi(pyren-1-yl)phosphine oxide ($POPy_2$) leads to a significant shift of the Fermi level toward the highest occupied molecular orbital and a 2 orders of magnitude increase in conductivity. Using CN6-CP and n-dopant (pentamethylcyclopentadienyl)(1,3,5-trimethylbenzene)ruthenium ($(RuCp*Mes)_2$), we fabricate a $POPy_2$-based rectifying p−i−n homojunction diode with a 2.9 V built-in potential. Blue light emission is achieved under forward bias. This effect demonstrates the dopant-enabled hole injection from the CN6-CP-doped layer and electron injection from the $(RuCp*Mes)_2$-doped layer in the diode.

KEYWORDS: *organic semiconductors, p-dopants, n-dopants, photoemission spectroscopy, p−i−n homojunctions, light emission*
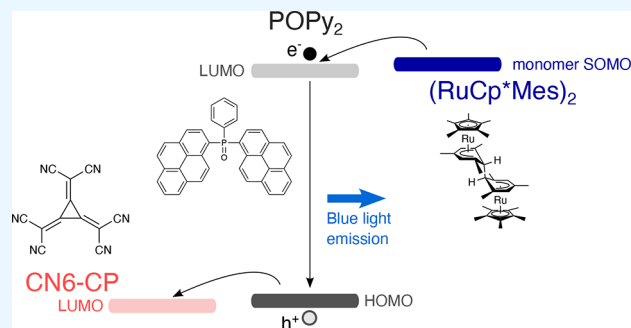
INTRODUCTION

Incorporating molecular dopants has proven to be a key method for improving the conductivity of, and charge injection into, organic semiconductors.[1−5] In the last two decades, various p- and n-dopants have been synthesized and characterized and have been shown to significantly improve charge transport properties in organic small molecules and polymers. p-Doping occurs when an electron is transferred from the highest occupied molecular orbital (HOMO) of the host material to the lowest unoccupied molecular orbital (LUMO) of the dopant, leaving behind a mobile hole, or positive polaron. In the case of a single-electron molecular oxidant, this process is, to the first approximation, energetically favorable when the electron affinity (EA) of the dopant is close to or higher than the ionization energy (IE) of the host material measured in the condensed state. This process becomes challenging when the IE of the host is large. Commonly used carbon-based molecular p-dopants, such as 2,3,5,6-tetrafluoro-7,7,8,8-tetracyanoquinodimethane (F$_4$-TCNQ, EA = 5.24 eV[6]), a fluorinated derivative of C$_{60}$ (C$_{60}$F$_{36}$, EA ∼ 5.40 eV[7]), 2,2′-(perfluoronaphthalene-2,6-diylidene)dimalononitrile (F$_6$-TCNNQ, EA = 5.60 eV[8]), and

molybdenum tris-[1,2-bis(trifluoromethyl)ethane-1,2-dithiolene] (Mo(tfd)$_3$, EA = 5.59 eV[9]), cannot efficiently p-dope hosts with IEs larger than ∼5.6 eV. This is a problem for hole injection in transport layers such as the ones used in green and blue organic light-emitting diodes (OLEDs), as these materials often have even deeper HOMO levels. Previous investigations have shown the use of the very high-EA molybdenum or tungsten trioxide (MoO$_3$, EA = 6.7 eV;[10,11] WO$_3$, EA = 6.5 eV[12]). Thermal evaporation of MoO$_3$ releases Mo$_3$O$_9$ (inorganic) trimers capable of p-doping organic materials such as 4,4′-bis(N-carbazolyl)-1,1′-biphenyl (CBP, IE ∼ 6.2 eV);[10] however, the high evaporation temperature and small size of the trimers present challenges in terms of damage and diffusion in organic molecular hosts. High-EA organic molecular dopants capable of p-doping large-IE materials
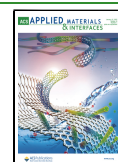
therefore remain of great interest. The strong molecular p-dopant hexacyano-1,2,3-trimethylene-cyclopropane (CN6-CP) is a promising candidate to address this issue.

Dianionic, radical-anion, and neutral forms of CN6-CP (molecular structure shown in Figure 1) were first reported by
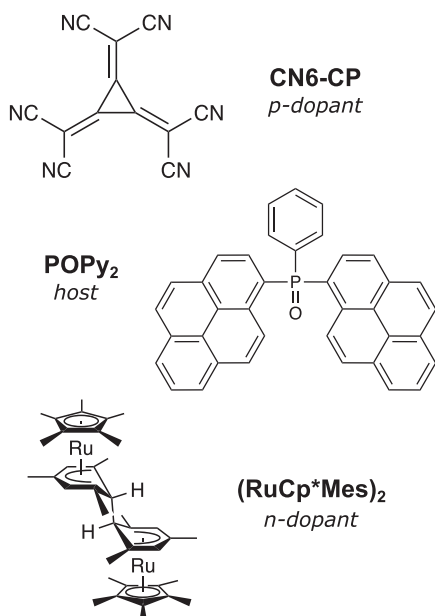

Figure 1. Molecular structures of CN6-CP, POPy$_2$, and (RuCp*Mes)$_2$.

researchers at DuPont in 1976[13,14] and have been investigated in conductive[14] and magnetic[15] charge-transfer salts and as components of magnetic coordination polymers.[16] The first use of a neutral molecule as a p-dopant for organic electronics was reported by Karpov et al.[17] in 2016, where it was used in suspension to p-dope a polymer, PDPP(6DO)TT, with a reported IE of 5.5 eV. Using cyclic voltammetry (CV), the EA of CN6-CP was estimated to be 5.87 eV. Karpov et al. also used CN6-CP$^{\bullet-}$ (estimated EA of 5.1 eV) as a p-dopant, with CN6-CP$^{\bullet-}$NBu$_4^+$ being highly soluble in a variety of organic solvents.[18] In the next section of this paper, we report the first measurement of the IE and EA of CN6-CP in the condensed phase using ultraviolet and inverse photoemission spectroscopy (UPS and IPES), respectively.

CN6-CP has also been processed through vacuum evaporation and has been used this way to p-dope pentacene[19] (IE = 4.94 eV[20]), copper phthalocyanine[21] (CuPc, IE = 5.35 eV[22]), 4,4′-cyclohexylidenebis[N,N-bis(4-methylphenyl)-benzenamine] (TAPC, IE = 5.50 eV), and tris(4-carbazoyl-9-ylphenyl)amine (TCTA, IE = 5.85 eV).[23] A much more soluble version of CN6-CP has been obtained by replacing three of the cyano groups by CO$_2$Me moieties, but it is a somewhat weaker p-dopant (estimated EA of 5.5 eV[24]). In this work, we use CN6-CP to p-dope phenyldi(pyren-1-yl)-phosphine oxide (POPy$_2$) (Figure 1), a large-band-gap material with a high IE (5.87 eV[25]) near the expected limit of the oxidation strength of CN6-CP. We measure the Fermi level (E_F) position, work function, and conductivity of the p-doped POPy$_2$ film as a function of the CN6-CP concentration.

Because of its large transport gap (3.6 eV), POPy$_2$ also has a small EA of 2.2 eV,[25] which makes n-doping highly challenging. We have previously demonstrated n-doping of

this organic semiconductor with (pentamethylcyclopentadienyl)(1,3,5-trimethylbenzene)-ruthenium dimer, (RuCp*Mes)$_2$ (Figure 1).[25] This dimer does not function as a single-electron reducing agent but contributes two electrons and undergoes bond cleavage to afford two monomeric cations.[26,27] Furthermore, in the case of POPy$_2$, the thermodynamic reducing strength of the dimer is estimated to be insufficient to result in an overall thermodynamically favorable reaction with this host. Photoexcitation of the host (under UV) or of the host:dimer charge-transfer state (under visible light) facilitates initial electron transfer from the dimer, immediately followed by cleavage of the dimer and release of a stable 18-electron cation RuCp*Mes$^+$ and a highly reducing 19-electron monomer. The latter then donates a second electron to the host.[25]

Given the possibility of achieving both p- and n-doping using these strong molecular oxidants and reductants in the large-gap, high-IE, and low-EA organic semiconductor POPy$_2$, we fabricate a p−i−n POPy$_2$ homojunction. To our knowledge, this type of homojunction has been realized to date with only three organic semiconductors, ZnPc (E_{gap} = 1.9 eV^2),[28] CuPc (E_{gap} = 1.8 eV),[22] and pentacene (E_{gap} = 2.1 eV),[29] all of which have significantly smaller IE and larger EA than POPy$_2$. The large POPy$_2$ transport gap (3.6 eV) gives the opportunity to achieve a much larger built-in potential than previously measured. We obtained blue light emission from this p−i−n diode.

■ EXPERIMENTAL SECTION

General Synthesis Details. All operations for the synthesis of CN6-CP and (RuCp*Mes)$_2$ were performed under an atmosphere of purified nitrogen, either using a standard Schlenk technique or in a glovebox. Acetonitrile was distilled over CaH$_2$, deoxygenated by three freeze−pump−thaw cycles, and stored inside a nitrogen-atmosphere glovebox. Trifluoroacetic acid was freshly distilled prior to use. The potassium salt of the CN6-CP radical anion (CN6-CP$^{\bullet-}$K$^+$) and (RuCp*Mes)$_2$ were prepared according to the literature methods.[17,30] All other reagents were purchased from Aldrich and used without any further purification. Mass spectra were recorded on an Applied Biosystems 4700 Proteomics Analyzer using ESI mode. Elemental Analyses were carried out by Atlantic Microlabs using a LECO 932 CHNS elemental analyzer.

Synthesis of CN6-CP. The compound was synthesized by modification of a published procedure.[17] CN6-CP$^{\bullet-}$K$^+$ (415 mg, 1.55 mmol) was taken in a Schlenk flask and dissolved in a minimum amount of acetonitrile (12 mL). To it, 6 mL of trifluoroacetic acid was added with vigorous stirring. NOPF$_6$ (350 mg, 2 mmol) was added to the above solution in one portion. After stirring for 3 h at room temperature, a yellow solid was formed. The solid was collected by filtration, washed with acetonitrile (3 × 2 mL), and then dried under high vacuum to obtain the desired product as a yellow-orange solid (328 mg, 93%). The solid slowly turned to dark green upon storing at room temperature or when in contact with some organic solvent vapors; however, the yellow-orange color of the compound can be maintained over weeks upon storage at −20 °C inside the glovebox. The CN6-CP synthesized for this work was stored in a freezer in the glovebox. For experiments, the CN6-CP was transferred from the freezer to ultrahigh vacuum (UHV) with minimal air exposure. ESI-MS (negative-ion mode): m/z 228.0 (M$^-$), 259.0 ([M + CH$_3$O]$^-$). Anal. Calcd. for C$_{12}$N$_6$: C 63.17, N 36.83, H 0.00; found: C 62.69, N 36.51, H 0.23.

Sample Preparation and Thin Film Deposition. All substrates were cleaned using the same method: 10 min sonication in acetone, then isopropanol, and 10 min of exposure to UV ozone. Substrates were then immediately transferred to UHV. The p-dopant (CN6-CP) and n-dopant ((RuCp*Mes)$_2$) were stored and evaporated in two

separate UHV chambers (both with base pressure of 10^{-9} Torr) to avoid cross contamination. $POPy_2$ (purchased from Lumtech) was also stored in each of these chambers so that it could be coevaporated with both dopants. The $POPy_2$ evaporation rate was maintained at 0.3 Å/s for all depositions. CN6-CP and $(RuCp*Mes)_2$ were evaporated at 0.1 and ∼0.03 Å/s, respectively.

Direct and Inverse Photoemission Spectroscopy. Samples were transferred without air exposure to the analysis chamber for photoemission spectroscopy measurements. UPS was used to characterize the occupied states of the undoped and doped organic films. The He I and He II lines (energies $h\nu = 21.22$ and 40.80 eV, respectively) emitted by a helium discharge lamp were used as the UV source. The unoccupied states in the films were measured using IPES, in isochromatic mode. The full setup for this technique is described elsewhere.[31] The experimental resolutions for UPS and IPES were 150 and 450 meV, respectively.

Conductivity Measurements. Patterned interdigitated electrodes were used to measure the lateral conductivity of the doped films. The 100 nm aluminum electrodes were evaporated in a thermal evaporator (Angstrom Engineering) through a shadow mask onto 1 cm × 1 cm quartz substrates cleaned in accordance with the parameters mentioned in the Sample Preparation and Thin Film Deposition section. The shadow mask had 16 thin alternating electrodes connected to a larger contact on either side, where every other thin electrode was electrically connected to one side and the other thin electrodes were connected to the opposite side. The gap between the thin electrodes was 150 μm, and the overlapping length of the thin electrodes was 0.5 cm. These substrates were loaded into the UHV system, where the films were evaporated and measured using a Keithley 2400 source meter.

Kelvin Probe Measurements. Contact potential difference (CPD) measurements on films deposited on ITO were conducted using a KP Technology UHV-KP020-50 Kelvin probe with a 5 mm diameter stainless steel tip in UHV. Highly ordered pyrolytic graphite (HOPG) was used as a reference sample for calibration. A freshly cleaved HOPG sample with minimal air exposure was loaded into vacuum and allowed to stabilize for ∼12 h. The work function of the HOPG was confirmed multiple times to be 4.7 eV using UPS, and the CPD of the HOPG was remeasured several times throughout the measurements of the CPD of samples with an unknown work function. The work function was calculated using equation $WF_{sample} = CPD_{sample-tip} - CPD_{HOPG-tip} + WF_{HOPG}$, where we assumed that WF_{tip} remains constant throughout the measurement.

Surface Photovoltage Measurements. SPV measurements were done with the Kelvin probe setup and LED and white lamp irradiation in UHV. The LEDs were from Thorlabs, 375 nm UV [M375L3] and 470 nm blue [M470L3], and the white lamp was an AmScope Series haloid lamp cold-light source [HL250-B].

Diode Measurements. Unpatterned 1 cm × 1 cm ITO/glass substrates were cleaned according to the sample preparation method mentioned previously. A thin layer of PEDOT:PSS was spin-coated on the surface (2000 rpm for 30 s, annealed at 150 °C for 10 min), and the substrate was transferred to UHV. CN6-CP p-doped $POPy_2$ was evaporated, and the chamber was pumped for at least 12 h before an undoped $POPy_2$ film was deposited to avoid unintentionally p-doping the undoped film. The sample was then transferred to another connected UHV chamber where the $(RuCp*Mes)_2$ n-doped $POPy_2$ was deposited. Ten minutes of UV irradiation was used to photoactivate the doping;[25] the sample was then left in UHV for at least 12 h to pump out the n-dopants before transferring the sample under inert atmosphere to a N_2 glovebox. Au contacts were deposited via thermal evaporation [Angstrom Engineering] at a base pressure of 10^{-7} Torr and a rate of 1 Å/s to a thickness of 100 nm. The devices were measured in the glovebox with lights turned off. A thin Au wire was used to make direct contact with the Au contact of the devices. Current−voltage characteristics were determined with a Keithley 2602B source meter.

UV−Vis−NIR Absorption Measurements. Absorption measurements were performed using an Agilent Technologies Cary 5000 UV−vis−NIR spectrometer. Quartz substrates were cleaned according to the process described previously.

Photoluminescence Spectroscopy. Photoluminescence was measured on a 50 nm thick $POPy_2$ film deposited on a quartz substrate [AdValue Technology]. A Newport TLS-300X tunable light source was used to excite the sample at 360 ± 10 nm. A high-resolution spectrometer [Princeton Instruments, Spectra Pro HRS-3000] with a CCD camera [Princeton Instruments, PIXIS 400B] captured the emission spectra. The sample was housed in a vacuum box during the measurement.

Electroluminescence Spectroscopy. Electroluminescence data was taken in a nitrogen-filled glovebox with a StellarNet Inc. fiberoptic spectrometer. The device was sourced with a Keithley 2602B source meter in a similar manner to the current−voltage measurement.

■ RESULTS AND DISCUSSION

To experimentally determine the IE and EA of CN6-CP, a 14 nm film was thermally evaporated onto a highly p-doped silicon (p^+-Si) substrate with a thin film of native oxide on the surface and measured using UPS and IPES in an ultrahigh vacuum (UHV) chamber. The experimental setup allows the film to be deposited and measured without exposure to air. The combined UPS/IPES data are shown in Figure 2. The EA
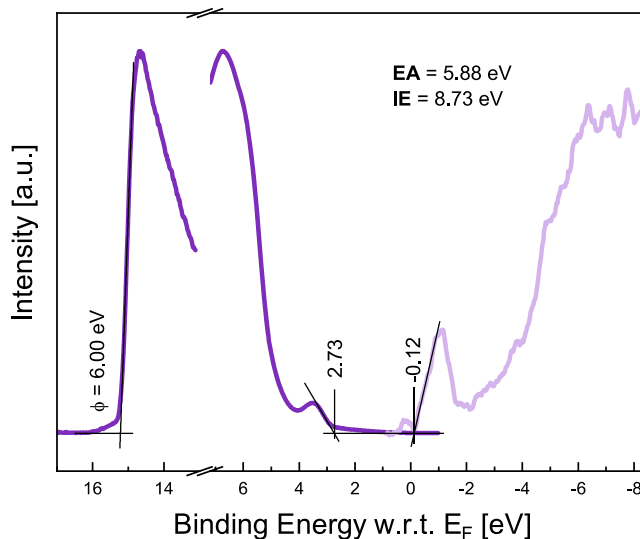
Figure 2. UPS He I (dark purple) and IPES (light purple) spectra of a 14 nm CN6-CP film deposited on p^+-Si. The energy differences between the E_F and the HOMO and LUMO are 2.73 and 0.12 eV, respectively, and the work function is 6.00 eV. Both the EA and IE of the film are reported.

and IE of the CN6-CP film are determined to be 5.88 and 8.73 eV, respectively. The work function of the film is 6.00 eV, with the E_F at 0.12 eV below the LUMO level. Since the EA of CN6-CP is larger than the Si substrate work function, there is electron transfer from Si to the film, accounting for the experimentally measured proximity of the E_F to the LUMO level. To the best of our knowledge, CN6-CP has the highest known EA to date for a neutral organic molecular p-dopant. We note that the EA measured here on the condensed CN6-CP film is in excellent agreement with that estimated via CV in the solution.[17]

With a low EA of 2.2 eV,[25] $POPy_2$ is typically used as an electron-transport material for injecting electrons into the LUMO level of green and blue OLED emissive layers.[32−34] While p-doping with CN6-CP has been shown to be efficient
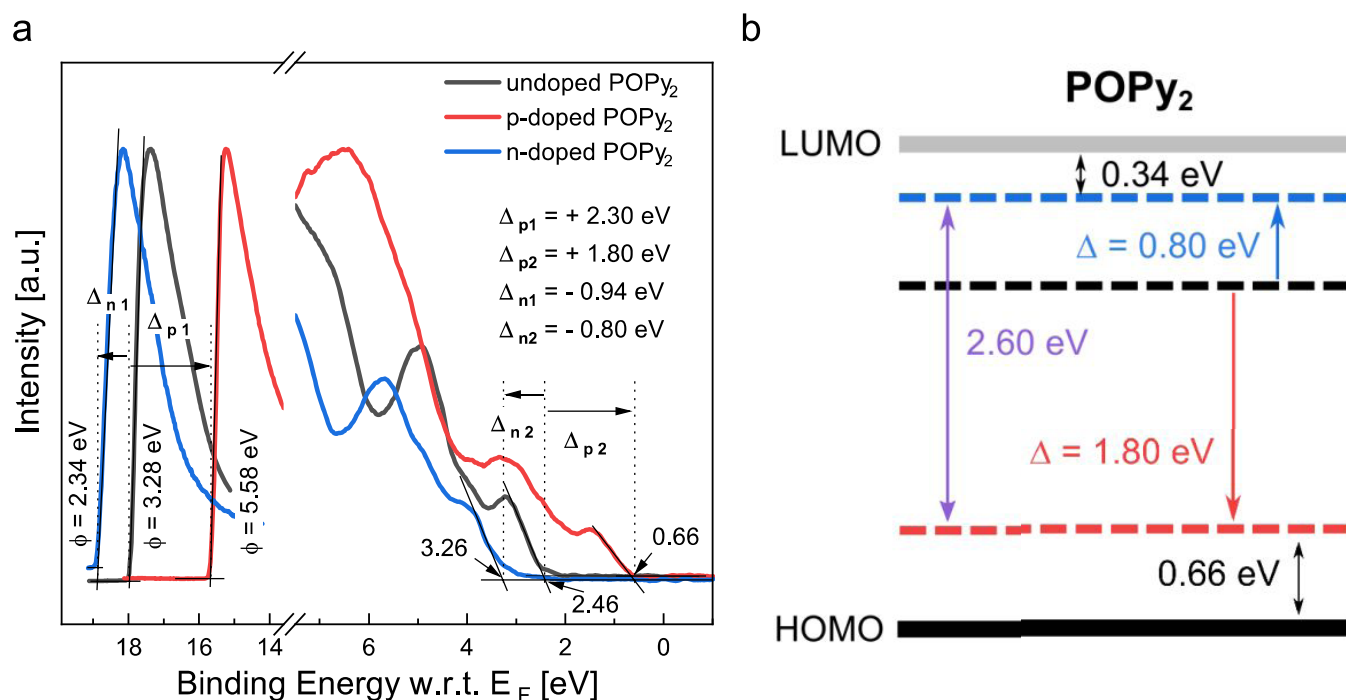
Figure 3. (a) Normalized UPS spectra of undoped POPy$_2$ [10 nm], 16% CN6-CP-doped POPy$_2$ (p-doped) [25 nm], and 10% (RuCp*Mes)$_2$-doped POPy$_2$ (n-doped) [10 nm], deposited on p-Si. The photoemission cutoff is measured with He I excitation. The HOMO and valence states are measured with He II excitation; the work function (ϕ) and HOMO edge position are given in each case. (b) Energy level diagram for POPy$_2$ showing the E_F position for the undoped (black), p-doped (red), and n-doped (blue) cases (dashed lines).

in high-IE hole-transport materials like TCTA[23] (IE = 5.85 eV), POPy$_2$ (IE = 5.8−5.9 eV) is an interesting material because it has already been shown to be n-doped using (RuCp*Mes)$_2$,[25] opening up the possibility of using these two strong p- and n-dopants to shift the E_F over a wide range of the 3.6 eV gap and fabricate a large built-in potential p−i−n structure.

The UPS spectra of Figure 3a show the effect of each dopant coevaporated with POPy$_2$ on p$^+$-Si (full details are provided in the Experimental Section). The undoped film (black spectrum) has a work function of 3.28 eV with the E_F at 2.46 eV above the HOMO edge. This yields an IE of 5.74 eV for POPy$_2$, close to the value of 5.87 eV reported by Lin et al.[25] A slightly higher IE of 5.9 eV was reported by Matsushima et al.[34] These small differences, which are within the 150 meV energy resolution of our UPS setup, are potentially due to morphological differences between films grown under different conditions and on different substrates.

When POPy$_2$ is p-doped with CN6-CP (red spectrum), the E_F shifts by 1.80 eV, toward the valence states, and reaches 0.66 eV above the HOMO level. The work function increases by 2.3 eV to 5.58 eV. Other doping concentrations and thicknesses of CN6-CP-doped POPy$_2$ films were also measured with UPS, as shown in Figure S1 in the Supporting Information. The work function increase is larger by 0.5 eV than the E_F shift, indicating an upward shift of the vacuum level (E_{vac}). This is presumably due to an accumulation of ionized (negatively charged) dopants near the surface, creating a surface dipole component. Correspondingly, the IE of the p-doped film, which from Figure 3a can be calculated to be IE = ϕ + (E_F − HOMO) = 5.58 + 0.66 = 6.24 eV, is 0.5 eV larger than that of the undoped film.

Upon n-doping with (RuCp*Mes)$_2$ (blue spectrum), the E_F shifts upward in the gap by 0.80 eV with respect to the

undoped film and reaches 0.34 eV below the POPy$_2$ LUMO. The work function decreases by 0.94 eV to 2.34 eV. Here again, the work function shift is 0.14 eV larger than the E_F shift, pointing to a corresponding lowering of the vacuum level, since the IE of the n-doped film, 5.60 eV, is 0.14 eV smaller than that of the undoped film. A schematic summarizing the movements of the E_F within the band gap of POPy$_2$ is given in Figure 3b. Most notable is the 2.60 eV difference between the p-doped and n-doped POPy$_2$ E_F positions, which demonstrates how these two strong dopants can be used to manipulate the E_F position in such a large gap material. However, E_F − HOMO (0.66 eV) is larger than expected in the p-doped film; this is puzzling given the oxidizing strength of the dopant, although gap states above the HOMO, the presence of which cannot be ruled out, could contribute to partial pinning the Fermi level at that position.

The conductivity of undoped and CN6-CP-doped POPy$_2$ was measured in UHV using an interdigitated electrode platform deposited on quartz, with a setup described elsewhere[35] (details are given in the Experimental Section). Note that the conductivity of POPy$_2$ doped with (RuCp*Mes)$_2$ has been previously characterized.[25] Because of its large transport gap (3.6 eV), intrinsic POPy$_2$ is practically insulating and it is difficult to measure its conductivity, which is estimated to be <10^{-10} S cm^{-1} (see Figure S2 for further details). Upon p-doping, the conductivity increases by approximately 2 orders of magnitude (Table 1). We note that this increase is relatively low for such dopant:host molar ratios. However, the not particularly close approach of the E_F position to the HOMO noted above is consistent with the relatively low conductivity achieved here, as the hole density is correspondingly low. Another potential factor that could limit the conductivity is that POPy$_2$ is typically employed as an electron-transport material due to its chemical structure.[32] The

Table 1. POPy$_2$ Conductivity vs CN6-CP Concentration, in Percent

% CN6-CP in POPy$_2$	Conductivity [S cm^{-1}]
0	$\sim 2 \times 10^{-10}$
5	2.3×10^{-8}
10	4.2×10^{-8}
25	7.5×10^{-8}

electron and hole mobilities are unknown due to the low conductivity of POPy$_2$ (Figure S2).

Using the undoped and doped materials characterized above, a p−i−n POPy$_2$ structure was built by sequential deposition of a p-doped POPy$_2$ layer (20 nm, 16% CN6-CP) on ITO, followed by an intrinsic POPy$_2$ layer (50 nm) and an n-doped POPy$_2$ layer (10 nm, 10% (RuCp*Mes)$_2$). Figure 4a shows the UPS He I spectra measured on the p-doped layer and the top n-doped layer of the p−i−n structure. Because undoped POPy$_2$ is insulating, and UPS requires thinner films when measuring insulating materials, we deposited p-doped, intrinsic, and n-doped films that were as thin as possible to avoid charging during UPS. This likely explains why the p-doped POPy$_2$ work function is slightly lower and the HOMO level is slightly farther away from the E_F than in Figure 3. Additionally, the photoemission cutoff from the top n-doped layer exhibits features that could indicate that the work function is even lower than 2.80 eV, but here, we fit the work function conservatively. Accordingly, the work function decreases by 2.29 eV (Δ_1) between the initial p-doped layer and the top n-doped layer. This work function shift corresponds to a movement of the E_F across the device from close to the HOMO level to close to the LUMO level of POPy$_2$ (Figure 4b). The rigid shift of the valence states with respect to the E_F is confirmed by nearly equal shifts of the HOMO level (Δ_3 = 2.38 eV) and of the next higher binding energy peak (Δ_2 = 2.35 eV). Figure 4b shows an approximate depiction of the shift of the E_F between the p-doped, intrinsic, and n-doped portions of the film. Since only the p-doped and n-doped portions of the p−i−n film were measured, the

molecular level shift shown here in the undoped film is an estimate. Finally, the feature trailing above the fitted HOMO level of the top n-doped layer is likely a contribution from the undoped POPy$_2$ film.

Photoemission spectroscopy on any semiconductor film, and in particular on a p−i−n structure of the type described above, can lead to surface photovoltage (SPV), a nonequilibrium condition. The SPV is generated by photoexcited carriers that accumulate on the surface of the film and induce a field that artificially shifts the E_F in the gap and tends to flatten the band/energy level bending. Looking at the schematic of the electronic structure of the p−i−n structure (Figure 4b), the impact of the He lamp UV source could, therefore, be to artificially decrease the measured built-in potential ($\sim$2.3 V) with respect to its value in the dark. To assess this issue and examine molecular level bending more closely, we used Kelvin probe-based contact potential difference (KP-CPD) and SPV measurements.

The work function measured via KP-CPD after the deposition of each film in the p−i−n structure (Figure 5a) is presented in Figure 5b. Unless specified, all measurements are conducted in the dark. The work function exhibits a large decrease between the p-doped POPy$_2$ layer ϕ = 5.4 eV [1], the intrinsic layer ϕ = 4.7 eV [2], and the n-doped layer ϕ = 2.5 eV [3c] (in the dark, after UV irradiation). The intermediate values [3a] and [3b] are specific artifacts of the doping activation process and SPV. Because the top n-doped film was kept in the dark during deposition and before the KP-CPD measurement, the work function ϕ = 3.9 eV [3a] did not decrease as much as could be expected with respect to the i-layer. Although the n-dopant was incorporated in the film, the doping process had not been photoactivated as is required for effective doping of POPy$_2$, as discussed previously. A second measurement [3b] of the work function was taken under UV LED irradiation, which decreased the work function slightly to 3.8 eV, but at this point, it was affected by SPV. Once the UV LED was turned off, the work function decreased to 2.5 eV [3c].
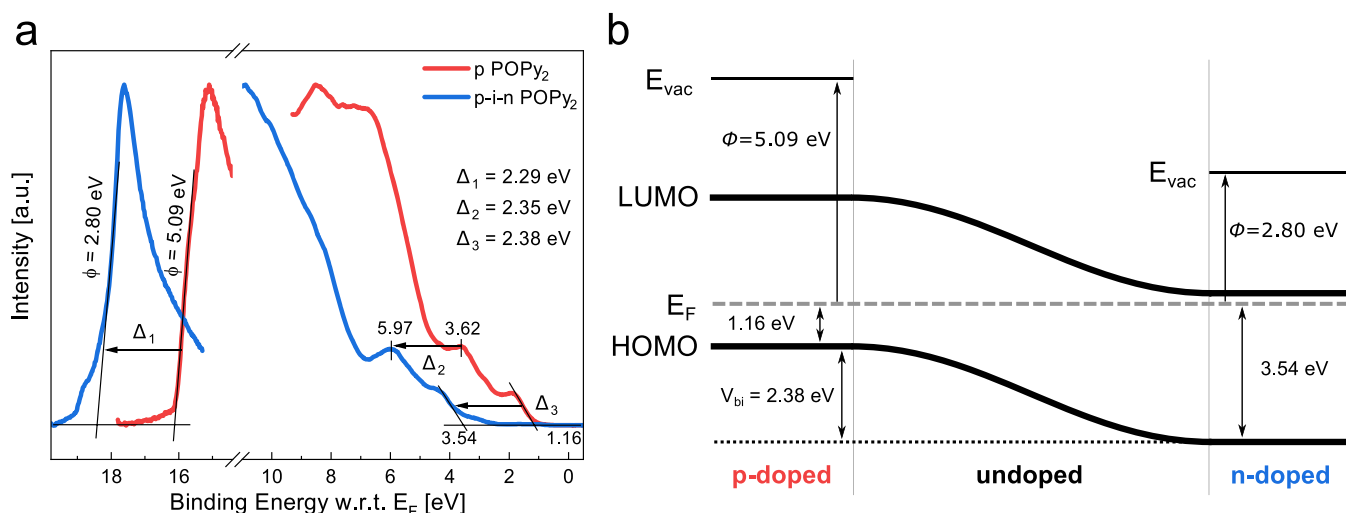

Figure 4. (a) Normalized UPS He I spectra of POPy$_2$ doped with CN6-CP (red) and of p−i−n POPy$_2$ on ITO with 16% p-doped POPy$_2$ (CN6-CP) [20 nm] (red)/undoped POPy$_2$ [50 nm]/10% n-doped POPy$_2$ (RuCp*Mes)$_2$ [10 nm] (blue), where the n-doped layer is on the surface. The photoemission cutoff and the valence state spectra show the rigid shift described in the text. (b) Schematic of the molecular level shift across the p−i−n POPy$_2$ film incorporating several parameters defined in (a), including the work function (ϕ), measured with respect to the vacuum level (E_{vac}) and distance between the Fermi level and HOMO for the p- and n-doped POPy$_2$ films, and the built-in voltage (V_{bi}) measured using UPS.
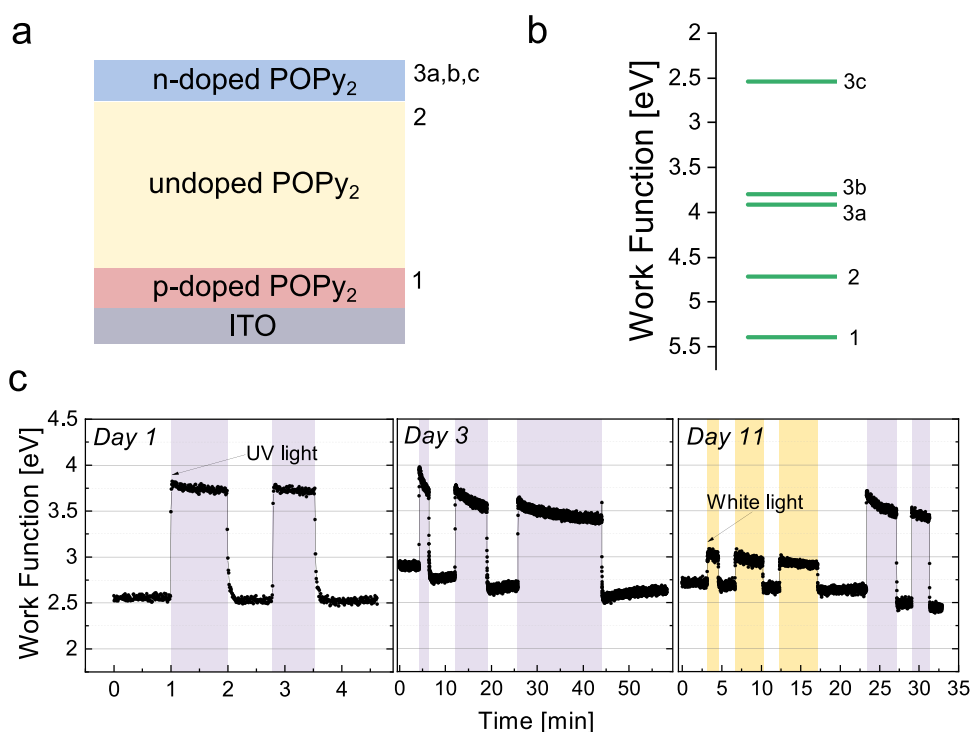
Figure 5. (a) Schematic of the p−i−n homojunction structure: ITO/p-doped POPy$_2$ (20 nm)/undoped POPy$_2$ (50 nm)/n-doped POPy$_2$ (10 nm). (b) Work function of POPy$_2$ measured by KP-CPD at various points in the process of depositing a p−i−n structure on ITO, starting with p-doped POPy$_2$ [1], then undoped POPy$_2$ on p-doped POPy$_2$ [2], and n-doped POPy$_2$ on undoped/p-doped POPy$_2$ with no previous light exposure [3a], irradiated with a UV LED [3b], and after irradiation [3c]. All measurements are done in the dark, except for [3b]. (c) Work function measurements showing surface photovoltage of the p−i−n POPy$_2$ structure. The structure was either kept in the dark, irradiated with UV light (purple shading) in portions of the first, second, and third (the second half) panels, or irradiated with white light (yellow shading) in portions of the first half of the third panel.

This KP-CPD experiment shows that the work functions measured in the dark on the p-doped layer (5.4 eV) and the top n-doped layer (2.5 eV) are larger and smaller, respectively, than the values measured by UPS for the p-doped layer (5.09 eV) and n-doped layer (2.80 eV) (Figure 4a). Therefore, the impact of SPV under the He discharge UV lamp appears to be particularly significant on the p−i−n structure, where the built-in potential measured in the dark is $1/e$ (5.4 − 2.5) = 2.9 V, where e is the charge of an electron, as opposed to the 2.3 V value obtained above from photoemission measurements.

The SPV measurements were conducted after the p−i−n structure was irradiated with UV to photoactivate the n-doping of the top POPy$_2$ film. At t = 0 min, the work function of the surface of the p−i−n structure kept in the dark was 2.5 eV (Figure 5b,c). We chose a UV LED (375 nm, 3.3 eV) for the SPV measurements since the optical gap of POPy$_2$ is 3.1 eV (Figure S3). At t = 1 min, the surface was irradiated with the UV LED and the work function increased to 3.7 eV, corresponding to an SPV of 1.2 V (Figure 5c, left panel). This measurement was repeated and the same work function change was obtained between dark and UV irradiation. The sample was also irradiated with a blue LED (470 nm, 2.6 eV), but the work function remained constant since this photon energy was below the optical gap of POPy$_2$ and thus unable to generate electron−hole pairs. The p−i−n structure was then stored in the dark in UHV, and the experiment was repeated 3 days later (Figure 5c, middle panel). The initial work function in the dark was 2.9 eV, but it gradually decreased following several irradiation sequences totaling ∼30 min, returning back to 2.5 eV. This presumably results from the reactivation of the

full doping process. In parallel, the initial work function upon UV irradiation was 3.9 eV, but it gradually decreased to 3.5 eV. Across these measurements on day 3, the SPV was slightly reduced from 1.2 V on day 1 to 0.9 V on day 3. Due to the sensitive nature of both the p- and n-dopants used in this film and/or to the expected sensitivity of the p- and n-doped POPy$_2$, it is possible that some degradation occurred, which led to the decrease in SPV. In addition, dopant diffusion in the p−i−n structure is a possibility, which would lead to a decrease in the thickness of the intrinsic region. Dopants were less likely to diffuse in amorphous films like POPy$_2$, and (RuCp*Mes)$^+$ was shown to be very stable in that material.[25] However, as the CN6-CP molecule is small, the possibility of diffusion cannot be excluded. The same structure was remeasured on day 11, first with a white lamp, which has a small contribution from wavelengths in the UV range, and then with the UV LED (Figure 5c, right panel). Upon illumination with white light (yellow shading), the work function increased from 2.7 to 3.1 eV, which is reasonable since the UV light coming from the white lamp is far less intense than that of the UV LED. When the sample was subsequently exposed to UV, the work function increased to 3.6 eV from 2.7 eV, giving an SPV of 0.9 V, comparable to what was observed on day 3.

Using a similar p−i−n structure, we fabricated a homojunction diode using thicker layers of p-doped (30 nm, 16% CN6-CP), undoped (200 nm), and n-doped (30 nm, ∼10% (RuCp*Mes)$_2$) POPy$_2$ deposited on PEDOT:PSS/ITO and using an Au top contact. The p−i−n film was fabricated in UHV and then transferred under N$_2$ to a glovebox equipped with a thermal evaporator to deposit the top contact and

measure the current−voltage characteristics of the diode. The current density vs voltage of the p−i−n structure is shown in Figure 6. The device exhibits a rectification ratio of more than
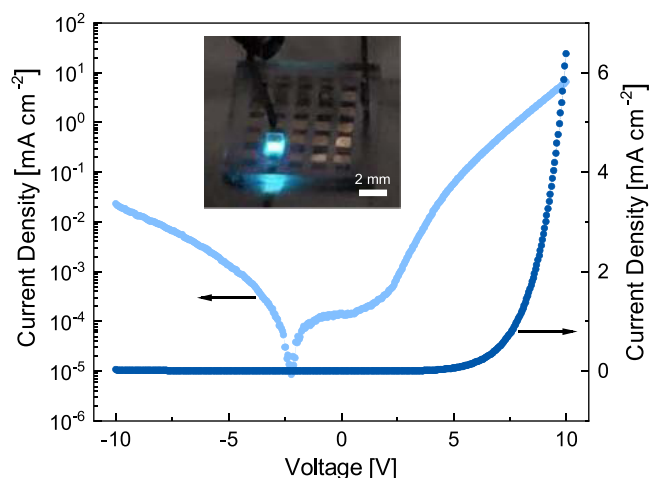

Figure 6. Current density vs voltage of the p−i−n diode, where the positive bias is applied to the ITO. The light blue data is on the log scale (left y-axis), and the dark blue data is on the linear scale (right y-axis). The inset image shows the emission of blue light from a device.

2 orders of magnitude at approximately 10 V (comparing forward to reverse bias). The same data were also displayed on a linear scale. When turned on at approximately 6 V, the device emitted blue light, shown in the inset of Figure 6. Furthermore, the photoluminescence (PL) spectrum of a POPy$_2$ film deposited on quartz and the electroluminescence (EL) spectrum collected from the p−i−n POPy$_2$ diode were in good agreement (Figure S4). The coincidence of the two demonstrates the bipolar operation of the diode and electrically pumped exciton recombination from POPy$_2$.

While POPy$_2$ is more commonly known as an electron-transport layer, as opposed to an emissive layer, it has been previously used in a single-layer organic light-emitting diode (SLOLED) by Matsushima et al.,[36] where it was blended with an orange fluorescent molecule, 2,5-bis[4-{bis(4-methoxyphenyl)amino}styryl]terephthalonitrile (BST). They fabricated undoped hole-only and electron-only devices with POPy$_2$ sandwiched between two contacts, but these devices did not emit light. Yet, in the present case, with the thin p-doped and n-doped layers ensuring efficient hole and electron injection, the forward-biased p−i−n device luminesces.

As a final note, we stress that the two contacts contained in the device, PEDOT:PSS/ITO on the p-doped side and Au on the n-doped side have typical work functions of ∼5.0 eV. Both are poorly matched for carrier injection in POPy$_2$, which exhibits extreme IE and EA of ∼5.8 and 2.2 eV, respectively. The fact that the device exhibits such a large built-in potential, as well as emitting light under forward bias, underscores again that heavily doped contacts render carrier injection nearly independent of the electrode electronic properties.

CONCLUSIONS

This work provides the first complete determination of the frontier energy levels of the powerful molecular oxidant CN6-CP using direct and inverse photoemission spectroscopy. We find the CN6-CP EA to be 5.88 eV, consistent with previous cyclic voltammetry measurements and the largest value currently known for an organic molecular p-dopant. We incorporate this dopant into a high-IE host, POPy$_2$, and demonstrate both an E_F shift closer to the HOMO level and a 2 orders of magnitude increase in the conductivity of the host film. We also use the previously studied powerful reductant (RuCp*Mes)$_2$ to n-dope POPy$_2$. With the ability to both p- and n-dope the large-band-gap POPy$_2$ (3.6 eV), we fabricate a p−i−n homojunction from sequentially vacuum-deposited layers and characterize each step using UPS and Kelvin probe contact potential difference. Using KP-CPD in the dark, we measure a 2.9 V built-in potential (80% of the gap). We then fabricate a p−i−n diode consisting of thicker layers and a top-deposited Au contact. The resulting p−i−n diode is found to be highly rectifying and to emit blue light under forward bias, demonstrating injection of both holes and electrons in the large-gap POPy$_2$ and recombination within the device. These experiments stress the importance of developing powerful oxidant and reductant molecular dopants to advance the field of large-energy-gap organic electronic devices.

ASSOCIATED CONTENT

Supporting Information

The Supporting Information is available free of charge at https://pubs.acs.org/doi/10.1021/acsami.1c21302.

UPS of different doping concentrations of CN6-CP in POPy$_2$ compared to neat films of CN6-CP and POPy$_2$, I−V curves of undoped POPy$_2$ and CN6-CP-doped POPy$_2$ at three different concentrations, absorption spectrum of undoped POPy$_2$, and photoluminescence and electroluminescence from POPy$_2$ (PDF)

AUTHOR INFORMATION

Corresponding Author

Antoine Kahn − *Department of Electrical and Computer Engineering, Princeton University, Princeton, New Jersey 08544, United States;* orcid.org/0000-0002-1612-3350; Email: kahn@princeton.edu

Authors

Hannah L. Smith − *Department of Electrical and Computer Engineering, Princeton University, Princeton, New Jersey 08544, United States;* orcid.org/0000-0002-7290-8865

Jordan T. Dull − *Department of Electrical and Computer Engineering, Princeton University, Princeton, New Jersey 08544, United States*

Swagat K. Mohapatra − *School of Chemistry and Biochemistry and Center for Organic Photonics, Georgia Institute of Technology, Atlanta, Georgia 30332, United States; Department of Industrial and Engineering Chemistry, Institute of Chemical Technology—Indian Oil Odisha Campus, IIT Kharagpur Extension Center, Bhubaneswar 751013 Odisha, India*

Khaled Al Kurdi − *School of Chemistry and Biochemistry and Center for Organic Photonics, Georgia Institute of Technology, Atlanta, Georgia 30332, United States*

Stephen Barlow − *School of Chemistry and Biochemistry and Center for Organic Photonics, Georgia Institute of Technology, Atlanta, Georgia 30332, United States; Renewable and Sustainable Energy Institute (RASEI), University of Colorado Boulder, Boulder, Colorado 80309, United States;* orcid.org/0000-0001-9059-9974

Seth R. Marder − *School of Chemistry and Biochemistry and Center for Organic Photonics, Georgia Institute of Technology, Atlanta, Georgia 30332, United States; Renewable and Sustainable Energy Institute (RASEI), University of Colorado Boulder, Boulder, Colorado 80309, United States; Department of Chemical and Biological Engineering and Department of Chemistry, University of Colorado Boulder, Boulder, Colorado 80309, United States;* ⓘ orcid.org/0000-0001-6921-2536

Barry P. Rand − *Department of Electrical and Computer Engineering, Princeton University, Princeton, New Jersey 08544, United States; Andlinger Center for Energy and the Environment, Princeton University, Princeton, New Jersey 08544, United States;* ⓘ orcid.org/0000-0003-4409-8751

Complete contact information is available at:
https://pubs.acs.org/10.1021/acsami.1c21302

Notes
The authors declare no competing financial interest.

■ REFERENCES

(1) Blochwitz, J.; Pfeiffer, M.; Fritz, T.; Leo, K. Low Voltage Organic Light Emitting Diodes Featuring Doped Phthalocyanine as Hole Transport Material. *Appl. Phys. Lett.* **1998**, *73*, 729−731.

(2) Gao, W.; Kahn, A. Controlled p-Doping of Zinc Phthalocyanine by Coevaporation with Tetrafluorotetracyanoquinodimethane: A Direct and Inverse Photoemission Study. *Appl. Phys. Lett.* **2001**, *79*, 4040−4042.

(3) Blochwitz, J.; Fritz, T.; Pfeiffer, M.; Leo, K.; Alloway, D. M.; Lee, P. A.; Armstrong, N. R. Interface Electronic Structure of Organic Semiconductors with Controlled Doping Levels. *Org. Electron.* **2001**, *2*, 97−104.

(4) Walzer, K.; Männig, B.; Pfeiffer, M.; Leo, K. Highly Efficient Organic Devices Based on Electrically Doped Transport Layers. *Chem. Rev.* **2007**, *107*, 1233−1271.

(5) Jacobs, I. E.; Moulé, A. J. Controlling Molecular Doping in Organic Semiconductors. *Adv. Mater.* **2017**, *29*, No. 1703063.

(6) Gao, W.; Kahn, A. Controlled p-Doping of the Hole-Transport Molecular Material N,N′-Diphenyl-N,N′-Bis(1-Naphthyl)-1,1′-Biphenyl-4,4′-Diamine with Tetrafluorotetracyanoquinodimethane. *J. Appl. Phys.* **2003**, *94*, 359−366.

(7) Yu, Y. J.; Solomeshch, O.; Chechik, H.; Goryunkov, A. A.; Tuktarov, R. F.; Choi, D. H.; Jin, J., il; Eichen, Y.; Tessler, N. p-Type Doping in Organic Light Emitting Diodes Based on Fluorinated C_{60}. *J. Appl. Phys.* **2008**, *104*, No. 124505.

(8) Zhang, F.; Kahn, A. Investigation of the High Electron Affinity Molecular Dopant F6-TCNNQ for Hole-Transport Materials. *Adv. Funct. Mater.* **2017**, *28*, No. 1703780.

(9) Qi, Y.; Sajoto, T.; Barlow, S.; Kim, E. G.; Brédas, J. L.; Marder, S. R.; Kahn, A. Use of a High Electron-Affinity Molybdenum Dithiolene Complex to p-Dope Hole-Transport Layers. *J. Am. Chem. Soc.* **2009**, *131*, 12530−12531.

(10) Kröger, M.; Hamwi, S.; Meyer, J.; Riedl, T.; Kowalsky, W.; Kahn, A. p-Type Doping of Organic Wide Band Gap Materials by Transition Metal Oxides: A Case-Study on Molybdenum Trioxide. *Org. Electron.* **2009**, *10*, 932−938.

(11) Meyer, J.; Hamwi, S.; Kroger, M.; Kowalsky, W.; Riedl, T.; Kahn, A. Transition Metal Oxides for Organic Electronics: Energetics, Device Physics and Applications. *Adv. Mater.* **2012**, *24*, 5408−5427.

(12) Hamwi, S.; Meyer, J.; Kröger, M.; Winkler, T.; Witte, M.; Riedl, T.; Kahn, A.; Kowalsky, W. The Role of Transition Metal Oxides in Charge Generation Layers for Stacked Organic Light-Emitting Diodes. *Adv. Funct. Mater.* **2010**, *20*, 1762−1766.

(13) Fukunaga, T. Negatively Substituted Trimethylenecyclopropane Dianions. *J. Am. Chem. Soc.* **1976**, *98*, 610−611.

(14) Fukunaga, T.; Gordan, M. D.; Krusic, P. J. Negatively Substituted Trimethylenecyclopropanes and Their Radical Anions. *J. Am. Chem. Soc.* **1976**, *98*, 611−613.

(15) Miller, J. S.; Ward, M. D.; Zhang, J. H.; Reiff, W. M. Structural and Magnetic Characterization of Electron-Transfer Salts of Hexacyanotrimethylenecyclopropanide, $\{C_3[C(CN)_2]_3\}^{\bullet-}$ and $[Fe-(C_5Me_5)_2]^{\bullet+}$ (1:1; Two Phases) and $[Fe(C_6H_3Me_3)_2]^{2+}$ (1:2). Evidence for 1-D Antiferromagnetic Behavior in Segregated $[Fe-(C_5Me_5)]^{\bullet+}$ Chains. *Inorg. Chem.* **1990**, *29*, 4063−4072.

(16) Kutasi, A. M.; Turner, D. R.; Jensen, P.; Moubaraki, B.; Batten, S. R.; Murray, K. S. Coordination Polymers of Hexacyanotrimethylenecyclopropanediide and Its Monoanionic Radical: Synthesis, Structure, and Magnetic Properties. *Inorg. Chem.* **2011**, *50*, 6673−6684.

(17) Karpov, Y.; Erdmann, T.; Raguzin, I.; Al-Hussein, M.; Binner, M.; Lappan, U.; Stamm, M.; Gerasimov, K. L.; Beryozkina, T.; Bakulev, V.; Anokhin, Dv.; Ivanov, D. A.; Günther, F.; Gemming, S.; Seifert, G.; Voit, B.; di Pietro, R.; Kiriy, A. High Conductivity in Molecularly p-Doped Diketopyrrolopyrrole-Based Polymer: The Impact of a High Dopant Strength and Good Structural Order. *Adv. Mater.* **2016**, *28*, 6003−6010.

(18) Karpov, Y.; Kiriy, N.; Formanek, P.; Hoffmann, C.; Beryozkina, T.; Hambsch, M.; Al-Hussein, M.; Mannsfeld, S. C. B.; Büchner, B.; Debnath, B.; Bretschneider, M.; Krupskaya, Y.; Lissel, F.; Kiriy, A. Sequentially Processed P3HT/CN6-CP$^{\bullet-}$NBu$_4^+$ Films: Interfacial or Bulk Doping? *Adv. Electron. Mater.* **2020**, *6*, No. 1901346.

(19) Xing, W.; Wu, S.; Liang, Y.; Sun, Y.; Zou, Y.; Liu, L.; Xu, W.; Zhu, D. Engineering the Doping Efficiency in Pentacene Thin Films for High Thermoelectric Performance. *ACS Appl. Mater. Interfaces* **2020**, *12*, 29540−29548.

(20) Lüssem, B.; Tietze, M. L.; Kleemann, H.; Hoßbach, C.; Bartha, J. W.; Zakhidov, A.; Leo, K. Doped Organic Transistors Operating in the Inversion and Depletion Regime. *Nat. Commun.* **2013**, *4*, No. 2775.

(21) Xing, W.; Chen, J.; Liang, Y.; Zou, Y.; Sun, Y.; Xu, W.; Zhu, D. Optimization of the Thermoelectric Performance of Layer-by-Layer Structured Copper-Phthalocyanine (CuPc) Thin Films Doped with Hexacyano-Trimethylene-Cyclopropane (CN6-CP). *RSC Adv.* **2019**, *9*, 31840−31845.

(22) Chan, C. K.; Zhao, W.; Barlow, S.; Marder, S.; Kahn, A. Decamethylcobaltocene as an Efficient n-Dopant in Organic Electronic Materials and Devices. *Org. Electron.* **2008**, *9*, 575−581.

(23) Liu, Y.; Nell, B.; Ortstein, K.; Wu, Z.; Karpov, Y.; Beryozkina, T.; Lenk, S.; Kiriy, A.; Leo, K.; Reineke, S. High Electron Affinity Molecular Dopant CN6-CP for Efficient Organic Light-Emitting Diodes. *ACS Appl. Mater. Interfaces* **2019**, *11*, 11660−11666.

(24) Saska, J.; Gonel, G.; Bedolla-Valdez, Z. I.; Aronow, S. D.; Shevchenko, N. E.; Dudnik, A. S.; Moulé, A. J.; Mascal, M. A Freely Soluble, High Electron Affinity Molecular Dopant for Solution Processing of Organic Semiconductors. *Chem. Mater.* **2019**, *31*, 1500−1506.

(25) Lin, X.; Wegner, B.; Lee, K. M.; Fusella, M. A.; Zhang, F.; Moudgil, K.; Rand, B. P.; Barlow, S.; Marder, S. R.; Koch, N.; Kahn, A. Beating the Thermodynamic Limit with Photo-Activation of n-Doping in Organic Semiconductors. *Nat. Mater.* **2017**, *16*, 1209−1215.

(26) Guo, S.; Mohapatra, S. K.; Romanov, A.; Timofeeva, T.; Hardcastle, K. I.; Yesudas, K.; Risko, C.; Brédas, J. L.; Marder, S. R.; Barlow, S. n-Doping of Organic Electronic Materials Using Air-Stable Organometallics: A Mechanistic Study of Reduction by Dimeric Sandwich Compounds. *Chem. Eur. J.* **2012**, *18*, 14760−14772.

(27) Guo, S.; Kim, S. B.; Mohapatra, S. K.; Qi, Y.; Sajoto, T.; Kahn, A.; Marder, S. R.; Barlow, S. n-Doping of Organic Electronic Materials Using Air-Stable Organometallics. *Adv. Mater.* **2012**, *24*, 699−703.

(28) Harada, K.; Werner, A. G.; Pfeiffer, M.; Bloom, C. J.; Elliott, C. M.; Leo, K. Organic Homojunction Diodes with a High Built-in Potential: Interpretation of the Current-Voltage Characteristics by a Generalized Einstein Relation. *Phys. Rev. Lett.* **2005**, *94*, No. 036601.

(29) Harada, K.; Riede, M.; Leo, K.; Hild, O. R.; Elliott, C. M. Pentacene Homojunctions: Electron and Hole Transport Properties and Related Photovoltaic Responses. *Phys. Rev. B* **2008**, *77*, No. 195212.

(30) Un, H. I.; Gregory, S. A.; Mohapatra, S. K.; Xiong, M.; Longhi, E.; Lu, Y.; Rigin, S.; Jhulki, S.; Yang, C. Y.; Timofeeva, T.; Wang, J. Y.; Yee, S. K.; Barlow, S.; Marder, S. R.; Pei, J. Understanding the Effects of Molecular Dopant on n-Type Organic Thermoelectric Properties. *Adv. Energy Mater.* **2019**, *9*, No. 1900817.

(31) Wu, C. I.; Hirose, Y.; Sirringhaus, H.; Kahn, A. Electron-Hole Interaction Energy in the Organic Molecular Semiconductor PTCDA. *Chem. Phys. Lett.* **1997**, *272*, 43−47.
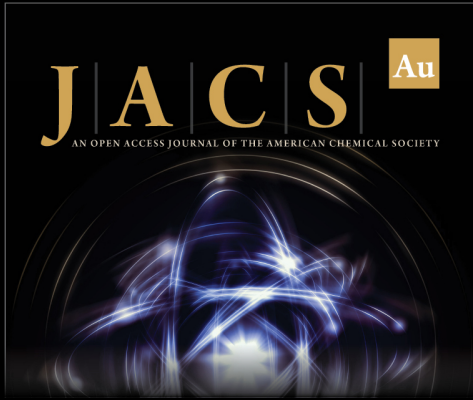
(32) Oyamada, T.; Sasabe, H.; Adachi, C.; Murase, S.; Tominaga, T.; Maeda, C. Extremely Low-Voltage Driving of Organic Light-Emitting Diodes with a Cs-Doped Phenyldipyrenylphosphine Oxide Layer as an Electron-Injection Layer. *Appl. Phys. Lett.* **2005**, *86*, No. 033503.

(33) Matsushima, T.; Adachi, C. High-Current Injection and Transport on Order of kA/cm^2 in Organic Light-Emitting Diodes Having Mixed Organic/Organic Heterojunction Interfaces. *Jpn. J. Appl. Phys.* **2007**, *46*, L861−L863.

(34) Matsushima, T.; Adachi, C. Suppression of Exciton Annihilation at High Current Densities in Organic Light-Emitting Diode Resulting from Energy-Level Alignments of Carrier Transport Layers. *Appl. Phys. Lett.* **2008**, *92*, No. 063306.

(35) Smith, H. L.; Dull, J. T.; Longhi, E.; Barlow, S.; Rand, B. P.; Marder, S. R.; Kahn, A. n-Doping of a Low-Electron-Affinity Polymer Used as an Electron-Transport Layer in Organic Light-Emitting Diodes. *Adv. Funct. Mater.* **2020**, *30*, No. 2000328.

(36) Matsushima, T.; Adachi, C. Bright Electroluminescence from Single-Layer Organic Light-Emitting Diodes Comprising an Ambipolar Carrier Transport Layer of Phenyldipyrenylphosphine Oxide. *Thin Solid Films* **2008**, *516*, 4288−4292.